Isotropic Connections Generate Functional Asymmetrical Behavior in Visual Cortical Cells

FLORENTIN WÖRGÖTTER, ERNST NIEBUR, AND CHRISTOF KOCH
Computation and Neural Systems Program 216-76, California Institute of Technology, Pasadena, California 91125

SUMMARY AND CONCLUSIONS

1. We study the relationship between structure and function in inhibitory long-range interactions in visual cortex. The sharpening of orientation tuning with "cross-orientation inhibition" is used as an example to discuss anisotropies that are generated by long-range connections.

2. In this study, as opposed to the detailed cortex model described in a previous report, a model of the cortical orientation column structure is proposed in which cortical cells are described only by their orientation preference.

3. We present results using different geometric arrangements of orientation columns. In the simplest case, straight parallel orientation columns were used. We also utilized more realistic, curved columns generated by a simple algorithm. The results were confirmed by the study of a patch of real column structure, determined experimentally by Swindale et al.

4. A given cell receives *functionally* defined cross-orientation inhibition if the cell receives inhibitory input that is strongest along its nonpreferred orientation. On the other hand, a cell is said to receive *structurally* defined cross-orientation inhibition if the inhibition arises from source cells with an orientation preference orthogonal to that of the target cell. Even though those definitions seem to describe similar situations, we show that, in the general case, structurally defined cross-orientation inhibition does not efficiently sharpen orientation selectivity. In particular, for straight and parallel columns, structurally defined cross-orientation inhibition results in unequal amounts of inhibition for whole cell populations with different preferred orientations.

5. In more realistic column structures, we studied the question of whether structural cross-orientation inhibition could be implemented in a more efficient way. However, for the majority of cells, it is demonstrated that their nonpreferred stimulus will not preferably excite "cross-oriented" cells. Thus structural cross-orientation inhibition is not efficient in real cortical columns.

6. We propose a new mechanism called *circular inhibition.* In this connection scheme, a target cell receives inhibitory input from source cells that are located at a given distance (the same for all cells) from the target cell. Circular inhibition can be regarded as two-dimensional long-range lateral inhibition. As opposed to structural cross-orientation inhibition, this mechanism does not introduce unwanted anisotropies in the orientation tuning of the target cells. It is also conceptually much simpler and developmentally advantageous. It is shown that this connection scheme results in a net functional cross-orientation inhibition in all realistic column geometries. The inhibitory tuning strength obtained with circular inhibition is weak and similar to that measured in reality.

7. Circular inhibition is isotropically arranged with respect to the target cell. Intriguingly, we find that it induces a directional bias in most of the cells regardless of the column structure. This effect is not due to noise-induced symmetry breaking but arises as an inherent feature of the functional architecture of visual cortex.

8. This study goes beyond approaches that describe cortical mappings in that it investigates the functional limitations imposed by interactions between intracortical connection schemes and the geometry of the column structure.

INTRODUCTION

The anatomic organization of the visual cortex lacks the strong ordering principles that are found in some other brain structures (e.g., retina, cerebellum). The functional organization, on the other hand, is highly ordered, and several functional elements have been discovered (e.g., ocular dominance, Hubel and Wiesel 1962; orientation columns, Hubel and Wiesel 1963, 1974; blobs and interblobs, Livingstone and Hubel 1984). Therefore the problem of linking low anatomic with high functional specificity has been of major research interest over the past years. Functional specificity can be achieved for excitatory interactions without any particular geometric relationship between the cells if their connections are strengthened by simultaneous activation (Hebb 1949; for a review see Kammen and Yuille 1990), which is a functional link. Pure Hebb mechanisms, however, do not work for interactions between inhibitory and excitatory cells. Thus a functional specificity in inhibitory mechanisms either has to be achieved in some other way or it might not exist. Recent experimental results partly support the second alternative (Bonds 1989).

By use of a detailed model of a part of the primary visual pathway, a previous study (Wörgötter and Koch 1991) showed how cortical cells could become orientation selective by a combination of low-specificity inhibitory mechanisms. It was observed that a certain type of more specific intracortical long-range inhibition (cross-orientation inhibition; Benevento et al. 1972; Burr et al. 1981; Sillito 1975) resulted in an unequal average orientation tuning for different populations of cortical cells. This finding triggered our interest in the functional implications of the geometric arrangement of the functional elements (the receptive fields).

In this study we will show that apparently isotropic cortical long-range connections contain inherent anisotropies and can result in functional asymmetries for different cells. Particularly, the "classical" cross-orientation inhibition scheme is subjected to functional limitations introduced by the cortical column structure. We propose a model in which inhibition arises isotropically from cells lying on a circle around the target cell ("circular inhibition"). Circular

inhibition can be looked on as two-dimensional long-range lateral inhibition. This model implements low structural specificity; it is conceptually simple and developmentally advantageous. We will demonstrate that the problems observed for cross-orientation inhibition will not occur for circular inhibition.

First, however, it is necessary to make clear what we mean by "cross-orientation inhibition," because this term is mostly used in the literature without a clear definition. Here, we will make a strict distinction between structurally and functionally defined cross-orientation inhibition (i.e., *structural cross-orientation inhibition* vs. *functional cross-orientation inhibition*). Structural cross-orientation inhibition will be used to denote the following geometric arrangement of receptive fields: a given orientation-selective cortical cell, called "target cell," receives inhibitory input from cells called "source cells" with an orientation preference that is orthogonal to that of the target cell. Functional cross-orientation inhibition, on the other hand, is defined by the actual inhibitory effect: a target cell receives the strongest inhibition for the *stimulus* orientation that is orthogonal to its own preferred orientation.

Note that neither definition contains any information about the relative topographical arrangement between source and target cell. This problem is one of the major topics of our study. We will show that the different definitions of cross-orientation inhibition, although apparently identical, actually describe quite different situations. In fact, structural cross-orientation inhibition will mostly not lead to functional cross-orientation inhibition. On the other hand, we will demonstrate that circular inhibition, which is only remotely related to structural cross-orientation inhibition, will nevertheless result in functional cross-orientation inhibition. Most intriguingly, circular inhibition, although it is a completely isotropic connection scheme, generates a directional bias, and hence an anisotropic effect, for most cells. Finally, we will discuss these results more broadly and draw conclusions about the general limitations of long-range connections.

At this point we wish to emphasize that we will concentrate on one aspect of cortical function, namely, the interac-tion between the geometric arrangement of the orientation columns and the synaptic connections [a much more realistic and complete model can be found in Wörgötter and Koch (1991)]. The model we introduce here is deliberately simple, and part of this study is devoted to a straight and parallel orientation column system because this can be treated analytically. At all stages of the study, however, we will show the similarity of those results with results obtained from more realistic cortical column structures and also from a patch of real cortex measured by Swindale et al. (1987).

RESULTS

Asymmetries in structural cross-orientation inhibition

In the first part of this section we will show that structural cross-orientation inhibition is subjected to certain functional limitations. To introduce the problem more clearly, we will proceed from a very unrealistic cortical model with straight orientation columns and rigid arrangement of the receptive fields to a more realistic version, which includes receptive-field scatter, overlap, and jitter in the preferred orientation, until we will finally treat a patch of a real cortex. The second part of this section will introduce and investigate circular inhibition as an alternative connection scheme.

Figure 1 shows how structural cross-orientation inhibition acts on two cells in a model cortex with parallel and straight orientation columns. The orientation columns are oriented vertically (Fig. 1*A*), and the small black bars represent the oriented receptive fields of the cortical cells. We assume a one-to-one projection from the visual field onto the cortex, which within small distances results in only a negligible error (Schwartz 1977, 1980; Tusa et al. 1978, 1979).

It is seen in Fig. 1 that cells with vertical and horizontal preferred orientation receive unequal amounts of inhibition when stimulated with their nonoptimal stimulus. The obvious reason is that a horizontal stimulus optimally covers the horizontally oriented inhibitory receptive fields in Fig. 1*B*, whereas the vertical bar does not cover the verti-
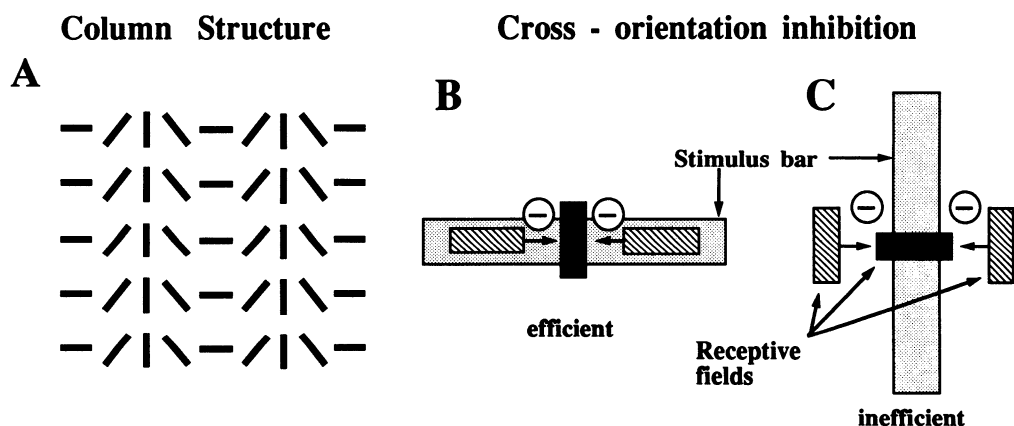

FIG. 1. Cross-orientation inhibition in an idealized column structure excluding receptive-field scatter and overlap. *A*: orientation column structure. Preferred orientations of cells in the model cortex. *B*: light bar (stippled rectangle) acting on the receptive fields of 3 cortical neurons. Receptive fields of 1 of them (*center* cell) is shown as a black rectangle. The other 2 neurons (shaded rectangles) provide inhibitory input (arrows) to the center cell. *C*: as in *B*, but at a different position in the column structure.
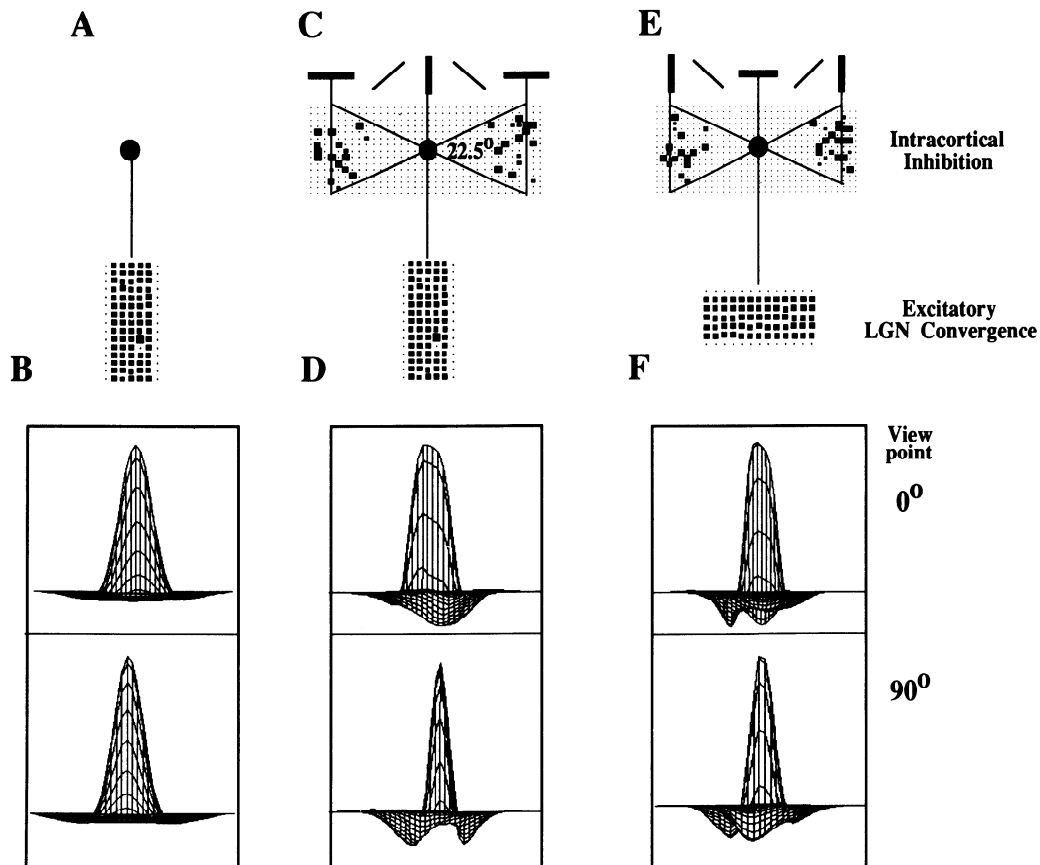
FIG. 2. Cross-orientation inhibition in an idealized column structure now including receptive-field scatter and overlap. *Top row*: the different connections to target cells indicated as large black dots. In *A*, the cell does not receive input from cortical cells, but only excitatory input from LGN cells. These are depicted in the *center row*. Each black square represents an LGN cell. *C* and *E*: center cell receives additional inhibitory input from cells at a distance of half a hypercolumn located within an angle of ±22.5°. The column structure is shown above the cortex cells. *B, D*, and *F*: receptive fields of the center cells shown in *A, C*, and *E*, seen along their long (*top*) and short axis (*bottom*), respectively.

cal receptive fields in Fig. 1*C*. Thus in these orientation columns structural cross-orientation inhibition works efficiently for vertically oriented receptive fields and inefficiently for horizontally oriented receptive fields of the respective target cell. Obviously, this effect has something to do with the fact that structural cross-orientation inhibition does not make any assumptions about the relative position of the connected cells within a column structure.

For the simplified column system in Fig. 1, the situation can be summarized as follows: efficient structural cross-orientation inhibition can only be achieved when the inhibitory receptive fields are aligned with the topographical representation of the stimulus that is nonoptimal for the target cell and (by definition) are orthogonal to the receptive field that is inhibited.

We will call such an alignment an *alignment along the cross-orientation axis*, because this axis is "cross-oriented" to the optimal stimulus orientation of the target cell. This, however, introduces the topographical relation between source and target cells as another parameter in the structural cross-orientation inhibition scheme. Before coming back to this more complicated issue (see Fig. 3), however, we first have to make sure that the observed anisotrophy is more than an artifact of the extremely simplified cortical model used so far.

Up to this point our model neglects the jitter in the orientation columns, receptive-field scatter as well as overlap (Albus 1975a,b). However, our detailed simulation (Wörgötter and Koch 1991) included those parameters, and we still found that structural cross-orientation inhibition will result in a significantly different orientation tuning of model cells with horizontal and vertical preferred orientation. Figure 2 shows the receptive fields of two cortical cells taken from the detailed simulation. The receptive fields were shaped by excitatory connections from the lateral geniculate nucleus (LGN; *center*) and then sharpened by inhibitory, intracortical connections (*top*; for details of the implementation see Wörgötter and Koch 1991). The first column of Fig. 2 shows a receptive field generated only by convergence from the LGN (Fig. 2, *A* and *B*). Each black square[1] in Fig. 2*A* represents the center of an LGN receptive field. The cortical receptive field (Fig. 2*B*) was computed by placing differences of Gaussians (DOG) on those centers and taking the sum of all DOGs at each point. The distance between the centers in the LGN was ~0.08°, and the DOGs had variances of $\sigma_{center} = 10.6'$ and $\sigma_{surround} = 31.8'$.

---

[1] The different sizes of the squares indicate the different axonal delays that have been used in the detailed cortex model (Wörgötter and Koch 1991), which, however, have no influence here.

Their ratio of center:surround amplitude was 17:1 (Enroth-Cugell and Robson 1966; for a recent review on the LGN see Casagrande and Norton 1990). Figure 2B presents the receptive fields along the preferred (top) and nonpreferred orientation (bottom). Comparison of these two views shows that the elongation of the receptive field for the model (using an aspect ratio of 13 × 5 LGN cells) is small compared with that of real cells.

The influence of structural cross-orientation inhibition is demonstrated for the same cell in Fig. 2, C and D. The intracortical connections and the column structure (similar to Fig. 1A) are shown in Fig. 2C. Cortical cells (black squares) within an angle of ±22.5° and at a distance of about half a hypercolumn are connected to the cell in the center. Each cortical cell has a receptive field (not shown) that is determined by its respective pattern of convergence from the LGN. To compute the receptive field of the cell in the center, we first computed for all cells the receptive fields as determined by the LGN convergence. The receptive fields of the inhibitory cortical cells were then subtracted with appropriate weights from the receptive field of the center cell. This process yields receptive fields with much larger elongation than those obtained with mere LGN convergence (Fig. 2D).

The same procedure was performed for a cell with horizontal preferred orientation (Fig. 2, E and F). The obtained structural cross-orientation inhibition is less efficient; it yields a smaller elongation (Fig. 2F) than for the vertically oriented field.

The data for Fig. 2 were taken from the detailed cortex model in which the receptive fields included realistic scatter, overlap, and jitter in the orientation columns. This shows that the asymmetry between cells with horizontal and vertical preferred orientations is not eliminated by realistic receptive-field arrangements.

In our model, cross-orientation inhibition has been implemented as subtractive inhibition. However, the arising asymmetrical behavior relies entirely on the shape of the receptive-field overlap and is not affected by the actual type of inhibition [subtractive vs. divisive (Blomfield 1974) or mixed from both types].

We will see in the following that the described effect is not an artifact generated by the artificial column structure we used.

Structural cross-orientation inhibition in a realistic column structure

Above we have stated that structural cross-orientation inhibition would work efficiently only if it actually arises along the so-called cross-orientation axis. In the following paragraph we will show that this is, in general, not the case in a real cortical column structure.

Figure 3A shows part of the cortical column structure from area 18 in the cat as measured by Swindale et al. (1987); the full structure is shown in Fig. 8A. The distance between hypercolumns found by these authors is about λ = 1.25 mm. Is it possible that, contrary to the case of straight columns, structural cross-orientation inhibition arises along the cross-orientation axis for a majority of cells in real cortex? Let us consider the three target cells in the thick circles. Straight lines are drawn through the centers of these cells that are orthogonal to their preferred orientations. Thus those lines are the topographical representation of stimuli along the cross-orientation axis. They are drawn stretching over approximately half a hypercolumn in both directions from the target cell. To be an efficient mechanism at that distance, structural cross-orientation inhibition should arise from source cells with orientations predominantly orthogonal to that of their target cell. The three
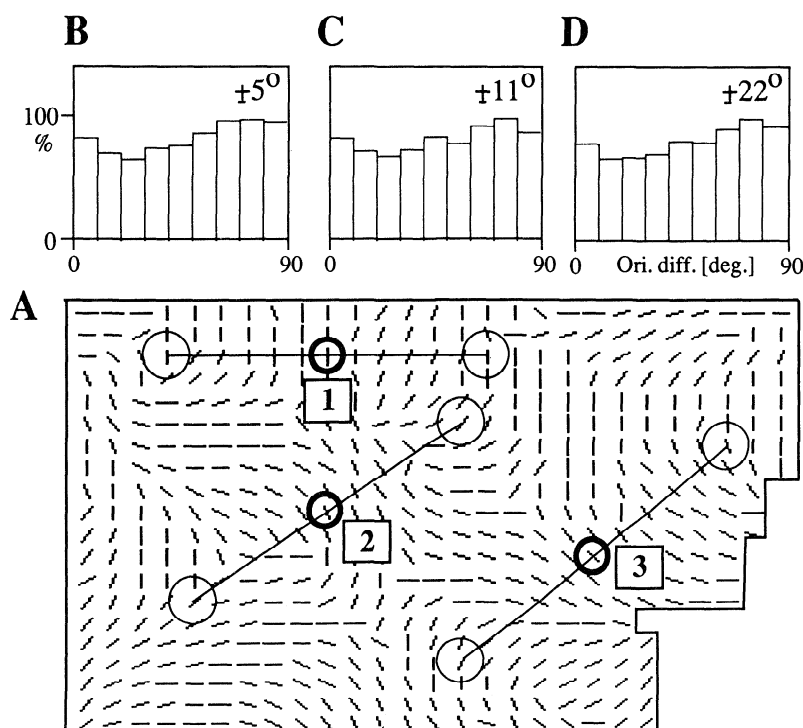

FIG. 3. Cross-orientation inhibition in a real cortical column structure. A: part of the orientational columnar structure in area 18 of cat [modified from Swindale et al. (1987) and shown more completely in Fig. 8]. Three target cells (in thick-lined circles) are depicted that get differently efficient cross-orientation inhibition. Cross-orientation inhibition arises from cells within the thin-lined circles that are located at the distance of half a hypercolumn and orthogonal to the preferred orientation of the target cell, i.e., at the end point of the "cross-orientation axis" (thin straight lines). B–D: distribution of the differences between the preferred orientation of source and target cells measured along the cross-orientation axis. Cross-orientation inhibition would be efficient if predominantly cells in the 90° bin were found. Distributions are measured within different angles around the cross-orientation axis: B, ±5°; C, ±11°; D, ±22°.

example cells show that this is not the general case. Cell 1 does not get any cross-orientation inhibition at that distance because the source cells (cells in the larger circles at the end of the line) are isooriented. Cell 2 gets efficient functional cross-orientation inhibition, whereas for cell 3 only the bottom connection contributes functional cross-orientation inhibition.

The efficiency of functional cross-orientation inhibition (obtained from structural cross-orientation inhibition) can be determined by measuring the difference between the preferred orientation of the target cell and the preferred orientations of source cells that lie on the cross-orientation axis. We have determined the distribution of those differences for all cells in the cortical column structure shown in Fig. 8, with the exception of those that are too close to the borders. Structural cross-orientation inhibition would work efficiently if most cells in the distribution have an orientation difference of 90° to their target (*rightmost* bin). To account for the receptive-field scatter, we measured distributions to determine the orientation differences between the respective target cells and all source cells within an angle around the cross-orientation axis. Figure 3, *B–D* shows three distributions measured at half a hypercolumn distance for angles ±5, ±11, and ±22°. The distributions are essentially flat with a small depression in the center. This shows that there is essentially an equal probability to find any orientation within small angles around the cross-orientation axis and at half a hypercolumn distance (i.e., $\lambda/2$). Similar distributions were obtained for distances between $\lambda/4$ and $3\lambda/4$ (not shown). This demonstrates that, within this range of distances, a restriction of the connection angle will result in an equal number of cells that get good, intermediate, or bad functional cross-orientation inhibition.

The analysis of structural cross-orientation inhibition in a real cortical patch so far assumed a one-to-one projection of the visual field onto the cortex, which was taken from area 18 (Swindale et al. 1987). Even though this is a reasonable assumption close to the area centralis, overall it is certainly an oversimplification because the topographical map in area 18 is continuous but distorted (Tusa et al. 1979). In our analysis this would result in a continuous deformation of the cross-orientation axis. We have determined the distribution of orientation differences in a similar way to that described above for a multitude of different locations around the center cells (data not shown).

For this patch of cortex we could not find a geometrically defined relation between source and target cells that would result in an overall efficient structural cross-orientation inhibition. In all cases with distances larger than $\lambda/4$ the distributions are essentially flat.

Structural cross-orientation inhibition could be implemented more efficiently if the connections along the cross-orientation axis were not all made at the same distance from the center cell, but at a distance where the orientation of the respective cell is optimal. This would, however, require the introduction of a supplementary parameter for each synaptic connection (the distance between the cells). Cell 1 shows that this would sometimes require rather long connections. Although this cannot be excluded, we will introduce in the following section a connection scheme that

has the virtue of being much simpler. It also eliminates the problems observed with cross-orientation inhibition and fits better to the inhibitory tuning curves measured experimentally.

Circular inhibition reduces structural asymmetries in intracortical long-range mechanisms

We return to the model cortex with parallel hypercolumns. Figure 4 shows the relation between receptive-field length and width for two cells taken from the detailed cortex model (Wörgötter and Koch 1991). One of the cells has vertical and the other one horizontal orientation preference. Both cells receive a similar connection pattern from the LGN. The spatial shape of the receptive fields was computed in the same way as for Fig. 2. The ratio R of receptive-field length versus width is determined at half of the peak height. Receptive-field plots have been normalized to the same peak height to account for the different number of cells that converge onto the center cell in Fig. 4. The ratio R is essentially identical for both cells when the receptive fields are generated only by LGN convergence (*leftmost* data points).[2] In the structural cross-orientation inhibition scheme, only cells within a small angle (here ±22.5°) are connected to the center cell. In this case, R is large for the cell with vertical preferred orientation; however, it stays at a low value for the other cell (compare Fig. 2). Increasing the angle within which the cells get their inhibition (±45 and ±90°) reduces R for the vertical cell and increases it for the horizontal cell until they are very similar if the inhibition arises from a full circle around the center cell. We call this *circular inhibition*. It reduces the asymmetry between the tuning strength of the cell populations with vertical and horizontal preferred orientation. Although the results for Fig. 4 were obtained with only static linear superposition of receptive fields, the same effects were reflected in the detailed cortex model. There, asymmetries between the tuning of vertically and horizontally oriented receptive fields occurred when structural cross-orientation inhibition was implemented and disappeared when circular inhibition was implemented.

Model for structurally induced tuning of inhibition

COMPUTATIONAL SCHEME. Computing the ratio of receptive-field length versus width for a large sample of cells and within more or less complicated column structures in the way shown for Figs. 2 and 4 is computationally expensive and does not necessarily yield insight into the underlying mechanism. Therefore, we present a model (see also APPENDIXES A and B) that captures the essential features introduced by the different column structures without unnecessary complexity. In an idealized circular inhibition scheme, the cell in the center of Fig. 5A receives input from all cells that are located exactly on the circle with half a hypercolumn radius ($\lambda/2$). Some of the receptive fields that contribute inhibition are shown below (Fig. 5B). The cell activity A is described as a function of the stimulus angle γ relative to the preferred orientation ϕ of the cell

---

[2] The slight difference results from 1 missing LGN connection in the cell with horizontal preferred orientation.
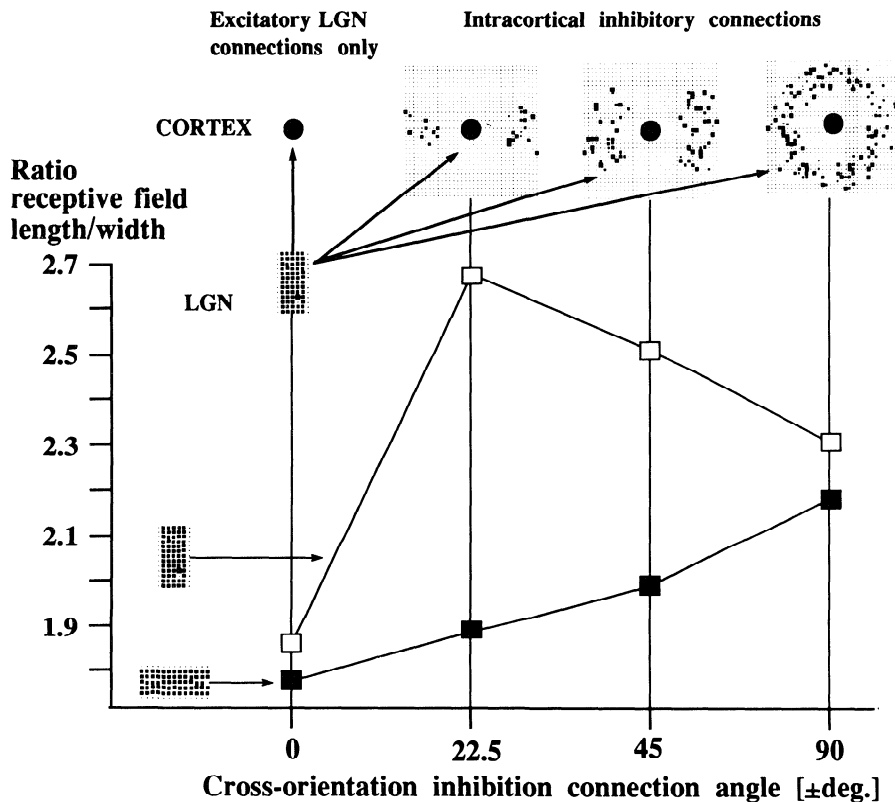
FIG. 4. Ratio between length and width of the receptive fields of cortical cells as function of the angle from which the cells receive intracortical inhibition. All cells receive excitatory input from the LGN. For the *leftmost* data point (0°), this is the only input. In all other cases, the inhibition arises from a distance of half a hypercolumn ($\lambda/2$). White (resp. black) data points: preferred orientation parallel (resp. orthogonal) to the columns. Circuitry for each data set is depicted above.

$$\mathcal{A}(\gamma - \phi) = A_0 + A_2\cos(2\gamma - 2\phi) \qquad (1)$$

This definition leads to simpler expressions than other shapes that we also implemented for the following computations. We used Eq. 1 because we found by computer simulations that the basic results are independent of the receptive-field shape, provided it is elongated, and because the constants A_0 and A_2 in Eq. 1 are the coefficients of the zero and second-order Fourier component [i.e., 0 and 2nd-order moment of a circular distribution (Batschelet 1981)] with which the orientation tuning of a cortical cell can be described rather accurately (Swindale et al. 1987; Thibos and Levick 1985; Wörgötter and Eysel 1987; Wörgötter et al. 1990). Thus the cell activity described by Eq. 1 can be directly associated with the measured peak activity that is obtained with a flashing bar at the different orientations. The small polar diagrams in Fig. 5B reflect this activity and their shape is similar to polar plots obtained in cells with orientation specificity but without direction specificity. Thus the shape of these polar plots does not correlate with the spatial shape of the receptive fields but with its orientation tuning curve. For simplicity we assume that all our model cells have the same degree of orientation tuning. Hence, values for A_0 and A_2 are constant and adjusted so that the ratio between long and short axes of the receptive field[3] $[(A_0 + A_2)/(A_0 - A_2)]$ is 3.33.

The activity of the cells on the circle (thick lines inside the receptive fields on the circle in Fig. 5B) gives an indication of the degree of inhibition that is elicited by a flashing δ-function bar[4] for the different stimulus orientations. The *tuning of inhibition* can then be computed by adding the activity values for all pairs of cells that face each other on the circle (see APPENDIX B, Eq. B5) and plotting it against the orientation angle in a polar diagram (Fig. 5C). Thus Fig. 5C shows the tuning of the circular inhibition (i.e., the strength of the inhibition and not the strength of the response as acted on by the inhibition) that a vertically oriented cell would receive in the column structure shown on *top* (Fig. 5A).

CIRCULAR INHIBITION FOR INDIVIDUAL CELLS. Figure 6 shows more examples of tuning curves for cells with preferred orientations as indicated on *top*. The tuning curves have been rotated to a common preferred orientation as indicated by the black bars in their centers. They have also been normalized to the maximum inhibition, which occurs only for the vertical and horizontal stimulus orientation in the cell in Fig. 6C. The unusual shape of the tuning curves is due to the lack of jitter in the column structure and the use of a δ-function bar. A bar with nonzero width will stimulate more than two cells on the circle.

The *bottom rows* of Fig. 6 show how the tuning curves change after introducing equally distributed random jitter of maximal ±20° in the orientation columns and using a bar width of 0.5°. The unphysiological cusps in the tuning

---

[3] This corresponds to an O-component of 53% or a half-width-at-half-height orientation tuning of $\sim 30°$. The empirical equation between O and half-width-at-half-height ($HWHH$) is (Wörgötter et al. 1990): $HWHH = 137.9 - 63.1 \times \log(O)$; the correlation r between $HWHH$ and O is better than 0.85.

[4] A δ-function bar is an idealization of an infinitely narrow stimulus bar.

A

Column structure

B

Computational scheme
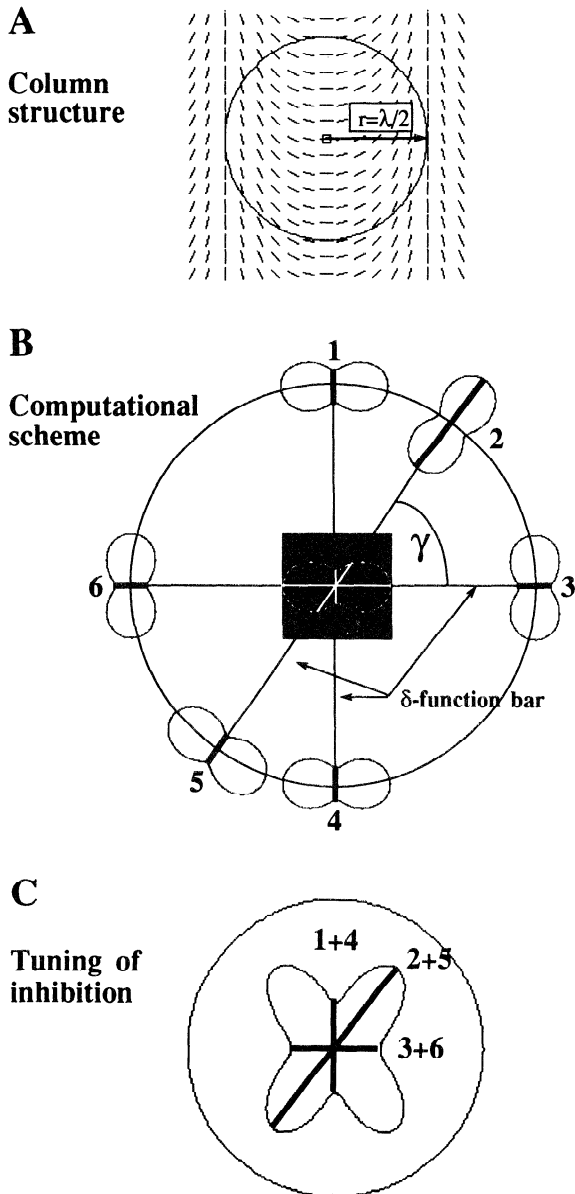

C

Tuning of inhibition

FIG. 5. *A*: computational scheme for the structurally confined model. Column structure of the model cortex defined in *Eq. B1*. Circular inhibition is implemented at a radius $r = \lambda/2$. *B*: effect of circular inhibition. *Center cell* receives input from all cells on a circle around it. Stimulus δ-function bars with angles 0, γ, and 90° excite cells 3 and 6, 2 and 5, and 1 and 4, respectively. *C*: polar plot of the tuning of inhibition received by the center cell (see *Eq. B5*).

curves disappear nearly completely and their shapes are comparable with those measured experimentally (Bonds 1989; Eysel and Wörgötter 1991). Two observations can be made: *1*) all tuning curves are weakly elongated, and *2*) the axis of elongation is in all these cases orthogonal to the preferred orientation of the respective cell.

We found the same result for cells of all orientations. Note that the examples shown span the whole range of $0 \leq \phi < 180$.

Because of the introduced jitter, there will be some cells that do not get tuned inhibition or that have a preferred axis of the tuning of inhibition aligned to that of the target cell.

The next section, however, will show that these cases are rare, so that the central result at this point is as follows:

The circular inhibition scheme yields weakly tuned functional cross-orientation inhibition on almost all cells.

Although Fig. 6 shows that realistic tuning curves are obtained for individual cells, we want to emphasize that the tuning of inhibition computed in this way gives only an indication of the influence of the column structure. We do not claim that our geometric model is able to reproduce the actual tuning of inhibition for a cortical cell, which not only depends on the geometry of the column structure but also on the inhibitory mechanism involved (e.g., subtractive vs. divisive).

INFLUENCE OF THE COLUMN STRUCTURE. In the qualitative survey of circular inhibition (previous section) we found that most of the cells receive weakly tuned functional cross-orientation inhibition. This was confirmed by computing the average tuning of inhibition that occurs within different column structures (Fig. 7).

Within each of the column structures, a sufficient[5] number of cells was selected yielding a constant distribution of preferred orientations. For each cell, the tuning of inhibition was computed as described in the sections above. The tuning curves were rotated to a common preferred orientation, and finally they were averaged (see APPENDIX B, *Eq. B6*). Because we were interested in the interactions between the column structure and the inhibitory mechanism, the averaging process was performed within ideal columns (without jitter in the orientations) and with a δ-function bar.[6]

Figure 7, *A* and *B* shows two control situations. The orientation column structure is in both cases highly unrealistic, as is the tuning of inhibition. A "cortex" with all receptive fields identical (Fig. 7*A*) will result in a rather sharp tuning of inhibition that is identical to the shape of the receptive fields itself (*Eq. 1*). This inhibition, however, is aligned to the receptive field of the target cell, i.e., it is not (functionally) cross-oriented but isooriented. We will come back to this result later (Figs. 8*B* and 10).

Not surprisingly, a cortex with randomly oriented receptive fields does not on average generate any tuned inhibition (Fig. 7*B*).

In Fig. 7, *C* and *D*, two similar-looking cortices are shown, which were generated as shown in APPENDIX A. The difference between the two cortices can be most easily seen in the one-dimensional plots of the orientation change shown on the *left* side of Fig. 7, *C* and *D*. The average tuning of inhibition achieved for the cortex in Fig. 7*C* is substantial, whereas the cortex in Fig. 7*D* does not produce any average tuning of inhibition at all.

---

[5] "Sufficient" means either 5,000 cells randomly selected from a cortex with 130,321 cells (Fig. 7, *B* and *E*) or 36 cells with 5° orientation difference between them (Fig. 7, *C* and *D*). For Fig. 7*A*, obviously only 1 cell needed to be chosen and no constant distribution of orientation can be achieved, because all orientations are identical.

[6] The averaging process results in a smoothing of the final tuning curve. Introducing additional jitter in the orientation columns and assuming wide bars as stimuli (as in Fig. 6) will essentially superimpose a 2nd smoothing process and not affect the results presented in the following.
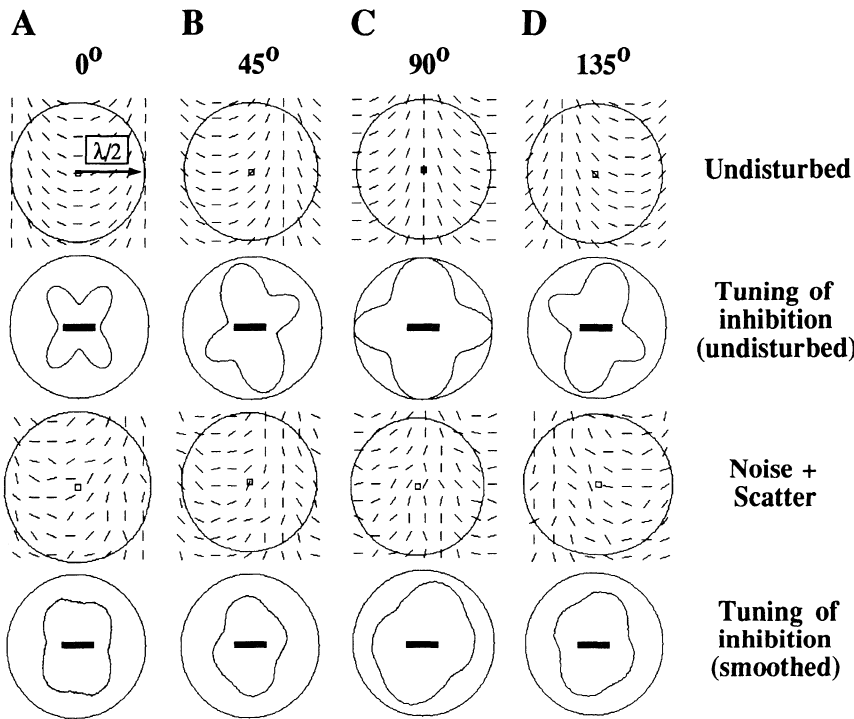
A   **B**   **C**   **D**

0°   **45°**   **90°**   **135°**

Undisturbed

Tuning of inhibition (undisturbed)

Noise + Scatter

Tuning of inhibition (smoothed)

FIG. 6. Circular inhibition obtained with a 0.5°-wide bar in a noisy column structure. Four cells are shown, with preferred orientations A, 0°; B, 45°; C, 90°; and D, 135°. *Top row* presents these cells in the undisturbed column structure. *Second row* plots their tuning of inhibition, obtained as demonstrated in Fig. 5. *Third row* represents the column structure after adding equally distributed orientation jitter of maximal ±20°. *Bottom row* shows the tuning of inhibition obtained in the noisy column structure and smoothed simulating stimulation with a wide bar.

The average tuning of inhibition in Fig. 7E was computed for the realistically curved column structure as shown in Fig. 12; it is lower than but still comparable with that shown in Fig. 7C.

AVERAGE TUNING OF CIRCULAR INHIBITION IN A REAL CORTEX. So far our results were obtained with artificial column structures. Figure 8A shows a part of the column structure of area 18 in a cat from the report of Swindale et al. (1987). Using circular inhibition, we determined the average tuning of inhibition as a function of the radius r of the circle (Fig. 8, B–G) by averaging over all cells for which the distance from all borders was at least r. We found that the most efficient functional cross-orientation inhibition
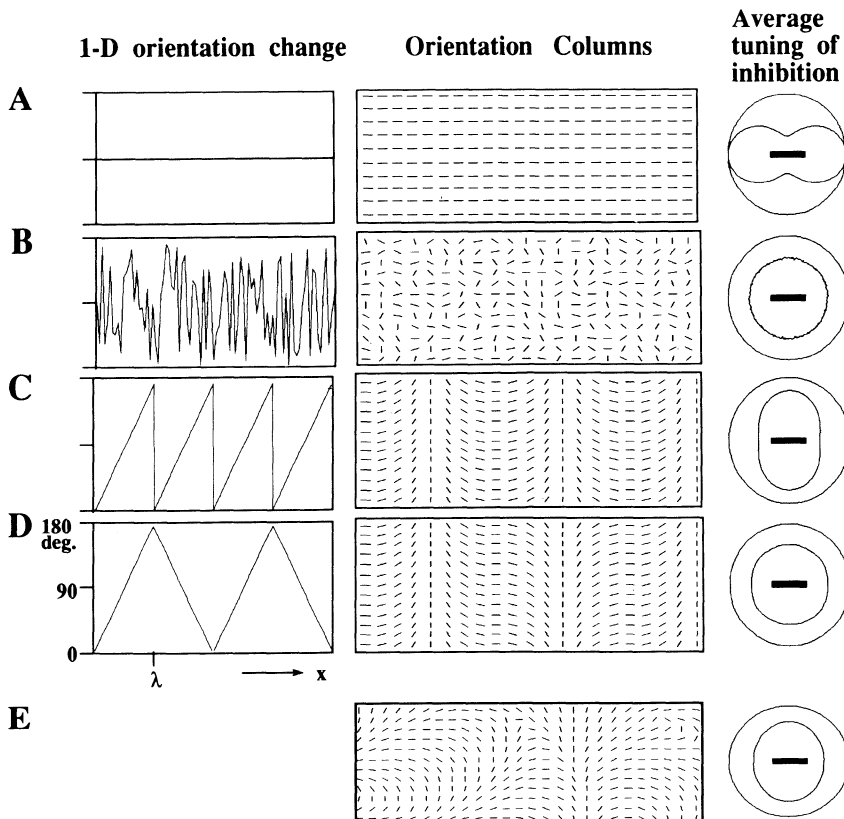
1-D orientation change   **Orientation Columns**   **Average tuning of inhibition**

A

B

C

D 180 deg.

90

0

λ   → x

E

FIG. 7. Population-averaged tuning of inhibition in 5 model cortices, using circular inhibition with r = λ/2. In A–D, the *leftmost* column shows the change of the preferred orientation along the horizontal (x-) axis. In A–E, the *center* column shows a part of the columnar structure, and the *rightmost* column the tuning of inhibition as polar plots. A: all preferred orientations parallel. Circular inhibition yields tuning with the same preferred orientation as the target cell. B: preferred orientations randomly distributed. No (i.e., isotropic) tuning of inhibition is obtained. C: column structure described by Eq. A2. A clear tuning of inhibition is observed, which is oriented orthogonal to the target cell. D: columnar structure with periodicity 2λ, obtained using the equation $\phi = \arctan|[\sin(\pi/\lambda\ x)]/[\cos(\pi/\lambda\ x)]|$. Although the structure looks very similar to that in C, no tuning of inhibition is obtained. E: realistic columnar structure defined by Eq. A3 with n = 3. Although the tuning of inhibition is less strong than in C, it is clearly present.
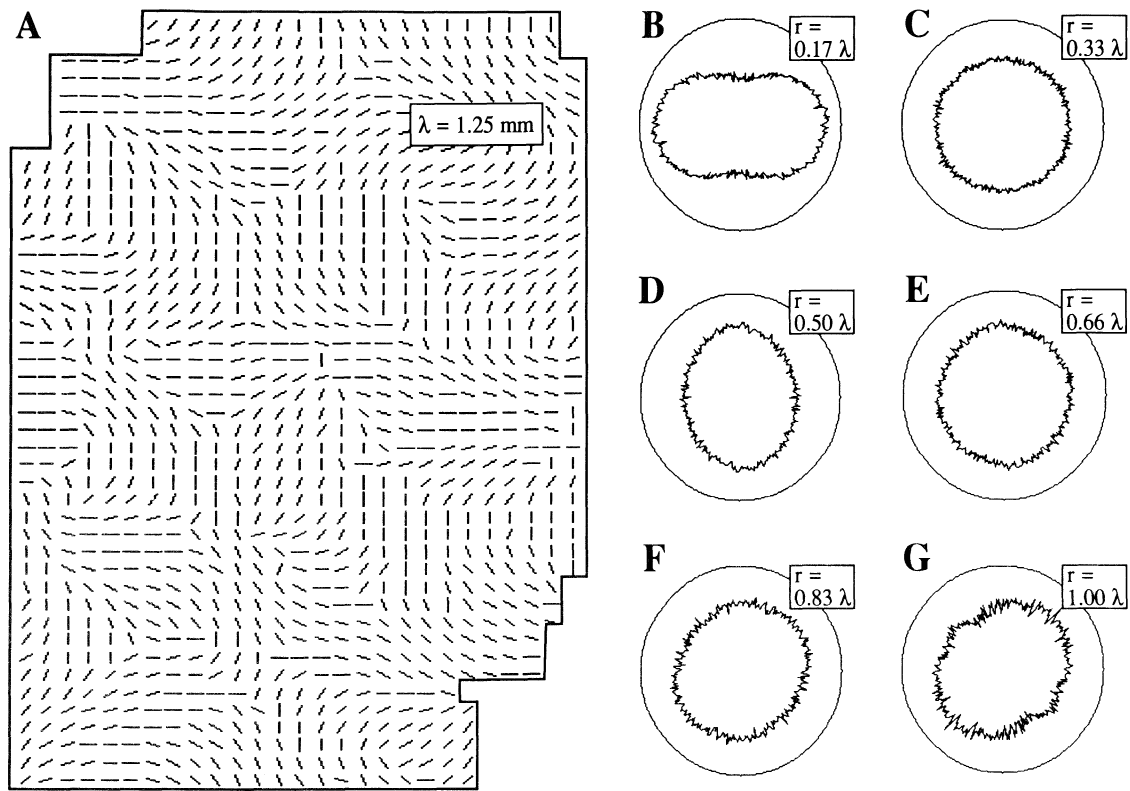
FIG. 8.   Circular inhibition in a real cortex. *A*: column structure in area 18 of a cat (modified from Swindale et al. 1987).
B–G: averaged tuning curves for different radii. Strongest net cross-orientation inhibition is obtained at $r = \lambda/2$.

(Fig. 8*D*) is obtained for $r = \lambda/2$ ($\lambda = 1.25 \pm 0.13$ mm; Swindale et al. 1987). For $r \to 0$, isoorientation interactions occur (Fig. 8*B*). A similar tendency seems to exist for $r \approx \lambda$ (Fig. 8*G*), although a clear tuning is not observed at this distance. This could be due to the rather small number of cells ($n = 59$) over which we could average to avoid border effect at this large radius. The results from a real cortex confirm the observations we made for our model cortices.

INFLUENCE OF THRESHOLDING.   So far, circular inhibition was generated by all cells on the circle. It is, however, more realistic to assume that inhibitory cells fire only if they are excited above a certain threshold. The effect of introducing a threshold on the average tuning of inhibition is shown for different cortices in Fig. 9. Figure 9, *C–E*, corresponds to the cortices shown in Fig. 7, *C–E*, and Fig. 9*S* corresponds to the real cortex shown in Fig. 8*A*. The threshold has been set to 1.5 times the minimum "activity" that can be generated by our artificial cells [i.e., $1.5 \times (A_0 - A_2)$ in *Eq. 1*].

The average tuning of inhibition is substantially strengthened by the thresholding for all cortices, which can be described by *Eq. A3*. Thresholding, however, has no effect for the cortex in Fig. 7, which does not follow this equation.[7]

INFLUENCE OF THE RADIUS.   The change of the tuning observed at different radii (Fig. 8) raised the question about

the relationship between the radius of circular inhibition and the actual shape of the tuning curves.

In the column structures discussed here, the average tuning curves have always an elongated shape with the long axis at either 0 or 90°. A measure of the efficiency of functional cross-orientation inhibition is the ratio between the average inhibition along the cross-orientation axis (I_{90}, Fig. 10) and the isoorientation axis (I_0). No tuning of inhibition exists if $I_{90}/I_0 = 1$ (Fig. 10, *inset 2*); cross-orientation inhibition is obtained if $I_{90}/I_0 > 1$ (Fig. 10, *inset 3*); and $I_{90}/I_0 < 1$ yields isoorientation inhibition (Fig. 10, *insets 1* and *4*).

The curves in Fig. 10 show how the average tuning changes for different column structures when r is varied. The letters marking the curves correspond to the cortices in Fig. 9. *Curve F* was obtained by the use of a cortex that obeys *Eq. A3* with $n = 2$.

"Isoorientation" inhibition is obtained in Fig. 7*A* and for $r \to 0$ (Fig. 10, *inset 1*) because the orientations of the target cell and the cells on the circle are similar at small distances.

The first maximum of the curves shows efficient functional cross-orientation inhibition. It is centered around $\lambda/2$.

Our theoretical approach can thus explain the experimental finding that strongest functional cross-orientation inhibition is obtained at a distance of about half a hypercolumn (Matsubara et al. 1985, 1987; Eysel and Wörgötter 1991).

Note that strongest average functional cross-orientation inhibition for the column structure shown in Fig. 7*C* (obeys *Eq. A3* with $n = 1$) is obtained for a radius larger than half a hypercolumn, $r \approx 0.65\lambda$ (*curve C*), whereas in *curve E* (*Eq. A3*, $n = 3$) the first maximum is shifted toward $\lambda/3$. For

---

[7] The tuning of inhibition obtained after thresholding in Fig. 9*C* is higher than the one observed in Wörgötter and Koch (1991). This difference stems from different elongations of the receptive fields used in the present study (3.33) and in that paper (1.78). The difference disappears if the same elongation is used (cf. Fig. 5*C*, *inset*).

curve F ($Eq.$ $A3$, $n = 2$), the maximum lies in between. The results from Matsubara et al. (1987) suggest that in area 18 strongest functional cross-orientation arises for $r \approx \lambda/2$ ($curve$ S). This corresponds to the maximum of $curve$ F, which is obtained with $n = 2$ in $Eq.$ $A3$. This is consistent with the observation that the power spectra of the cortical column structures from Swindale et al. (1987) seem to have two peaks (see Fig. 9 there). In fact, the number of peaks in the power spectra shown in this report (Swindale et al. 1987) is directly related to n in $Eq.$ $A3$.

Minima of I_{90}/I_0 (yielding isoorientation effects) are found, depending on the detailed column structure, when r is close to λ (Fig. 10, $inset$ 4). Although so far we have always discussed inhibitory interactions, there is obviously no reason to assume a priori any particular "sign" for the effect of circularly arranged connections. There is substantial experimental evidence for excitatory connections that stretch over a full hypercolumn (Gilbert 1985; Gilbert and Wiesel 1983; Nelson and Frost 1985; Rockland and Lund 1982, 1983; Ts'o et al. 1986), which could strengthen the

FIG. 10. Ratio I_{90}/I_0 between input arising along (I_{90}) and across (I_0) the cross-orientation axis as a function of the radius of circular inhibition. Labels are used according to the cortices in Fig. 7 from which the curves are obtained. Curve C is the exact result, calculated in APPENDIX B ($Eq.$ $B7$). Curves E and F are obtained from the model cortices defined in $Eq.$ $A3$, with: E: $n = 3$ ($k_1 = 0, l_1 = 1, k_2 = \sqrt{3}/2, l_2 = 1/2, k_3 = 1, l_3 = 0$). F: $n = 2$ ($k_1 = 0, l_1 = 1, k_2 = 1, l_2 = 0$). Curve S is computed using the experimentally observed data from Swindale et al. (1987), presented in Fig. 8A. Insets: polar plots of the tuning of inhibition for characteristic values of r, obtained from $Eq.$ $B6$.
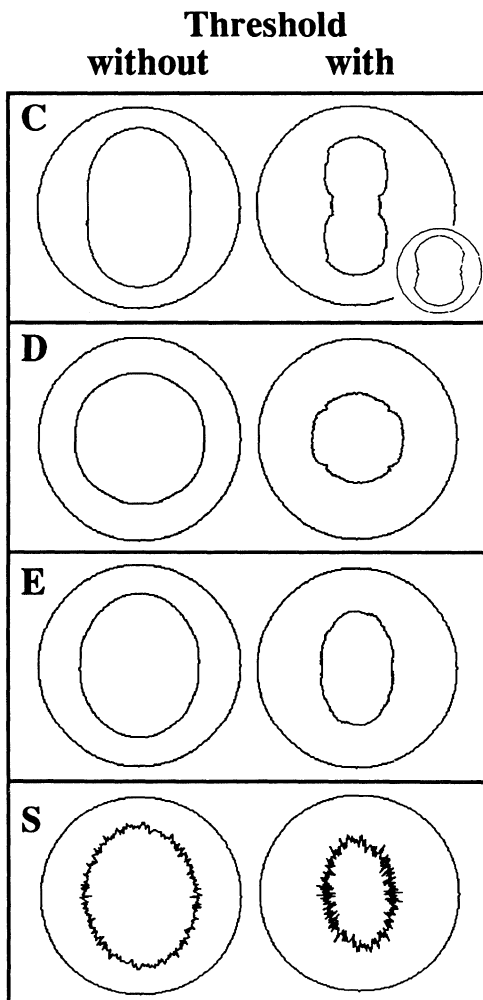
Threshold
without   with

FIG. 9. The effect of thresholding on circular inhibition. Polar plots showing the tuning of inhibition are presented for different cortices. The same labels as in Fig. 7 are used. (S) refers to the real cortical column structure as measured by Swindale et al. (1987).
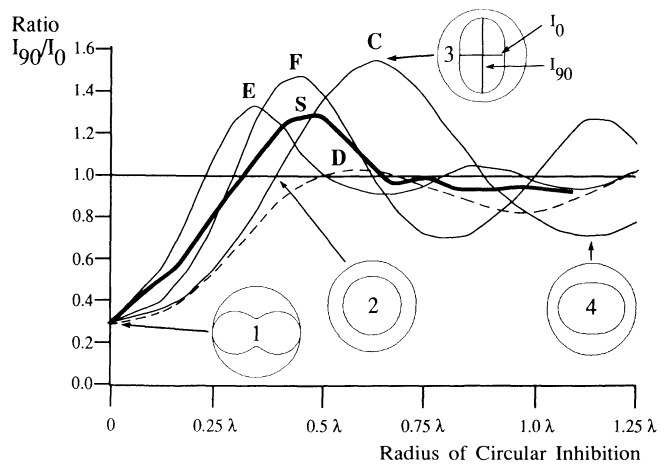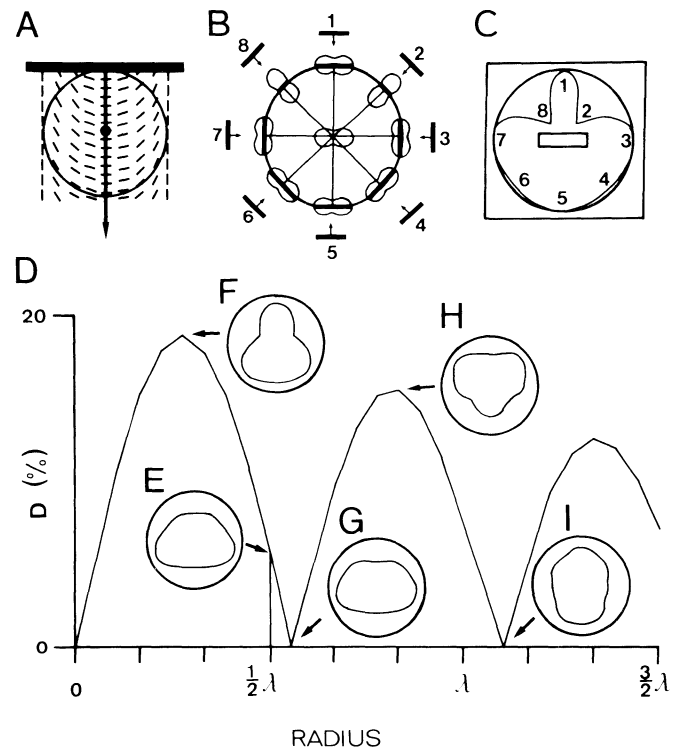

FIG. 11. Generation of a directional bias by circular inhibition in parallel orientation columns. A: δ-function bar (horizontal bar) moving over the model cortex defined by $Eq.$ $B1$. Circle shows the radius of circular inhibition ($r = \lambda/2$). B: Computational scheme for the tuning of inhibition received by the center cell, which has a horizontal preferred orientation. C: tuning of inhibition for the center cell. D: radius dependency of the average tuning of inhibition for the whole cell population in the column structure shown in A. The directional tuning coefficient D is calculated using SDO-analysis (Wörgötter et al. 1990) and plotted as a function of the radius of the circle of inhibition. Before averaging, tuning curves were rotated to a common preferred direction. Insets E–I: average tuning of inhibition at selected radii.
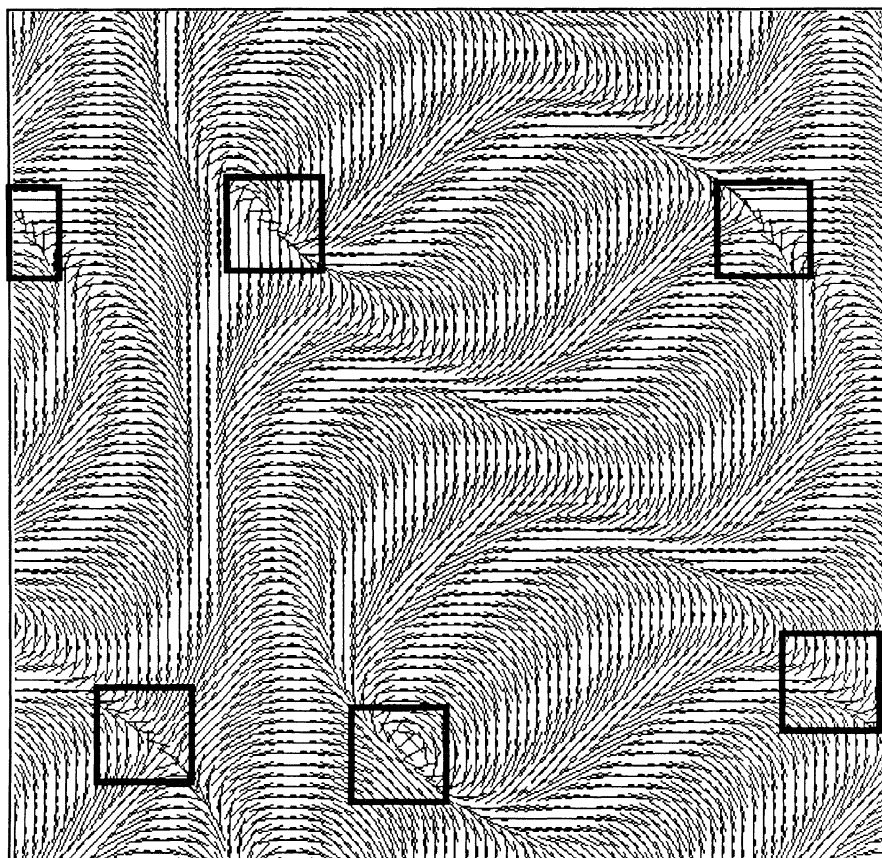
FIG. 12. Orientation column structure in a model cortex defined by *Eq. A3*, for $n = 3$ with: $k_1 = 0$, $l_1 = 1$, $k_2 = \sqrt{3}/2$, $l_2 = 1/2$, $k_3 = 1$, $l_3 = 0$. Black squares denote areas where the orientation changes discontinuously.

orientation tuning (Nelson and Frost 1985). Long-range inhibitory interactions have also been reported (Eysel et al. 1988; Somogyi et al. 1983). These can have an effect on the directional tuning if they are not isotropic (e.g., if more inhibition arises from one side than from the other). Because inhibitory and excitatory cells exist in all cortical columns, it is conceivable that both inhibitory and excitatory connections occur at the distance of a hypercolumn, and our results show that such connections will on average result in an isoorientation interaction.

The broken curve (Fig. 10D) belongs to the column structure shown in Fig. 7D. Very small tuning is obtained for this cortex, except for the isoorientation tuning for $r \rightarrow 0$, which is a (trivial) consequence of the local continuity of the orientation columns.

Generation of a directional bias

In a previous study (Wörgötter and Koch 1991) we found that circular inhibition can result in a directional bias, which is an anisotropic effect, even though circular inhibition is an isotropic connection scheme. In this section we will provide an explanation for this behavior.

The directional tuning of a cortical cell is (Kato et al. 1978; see also Orban 1984) the difference between the responses for motion in the two directions along the axis that is orthogonal to the preferred orientation of the cell. For appropriate temporal interactions between source and target cells, directional tuning is obtained if the net (excitatory

or inhibitory) effect is stronger along one of the two directions.[8]

We assume that the inhibitory input to the target cell arises from that cell on the circle that is excited first by the moving stimulus bar (see Fig. 11B). Furthermore, we will not deal with more realistic temporally induced effects other than assuming that the inhibition arising from this source cell will arrive within an appropriate time window together with the activation of the center cell.

The tuning curve for the center cell computed for all directions of motion is shown in Fig. 11C; corresponding points in Fig. 11, B and C are indicated by numbers. The tuning curve exhibits a strong asymmetry with respect to the horizontal preferred orientation, which results in a directional bias of $D = 26\%$ [$DI = 48\%$]. Note that identical amounts of inhibition will be elicited along both the downward (1) and the upward (5) direction of motion. A similar situation occurs for all cells in a straight-line parallel column structure. This symmetry, however, occurs only in a straight column structure. In curved columns, cells on the circle and arranged along the axis of preferred motion will

---

[8] Direction tuning is commonly measured with the direction index DI [for a definition see Orban (1984)]. Wörgötter and Eysel (1987) introduced a more reliable measure, called SDO-analysis (see also Batschelet 1981; Swindale et al. 1987; Thibos and Levick 1985; Wörgötter et al. 1990). Because SDO-analysis is not widely used, the D (direction) values from SDO-analysis will be followed in the text by DI values in brackets []. DI is computed from D by the following empirical equation: $DI = 60.9 \log_{10} (D) - 38.7$

virtually always have different orientations, and the inhibitory impact will consequently be different for both directions. Including jitter in the orientation column system will even eliminate this "singular" point in the straight column structure. Thus, the central result at this point is that a directional asymmetry is obtained from isotropic connections.

Figure 11D shows the radius dependency of the average directional bias. Tuning curves for all cells in the straight column structure have been rotated to a common preferred direction and averaged before computing their D values. The insets ($E-I$) show the averaged tuning curves for different example radii.

The average asymmetry between the tuning curves is considerable and would result in a direction bias of maximally $D = 19\%$ [$DI = 39\%$], which is more than one-half the average directional bias observed in simple cells, which is $\sim DI = 50\%$ (Berman et al. 1987; Orban 1984). Note, however, that the strongest directional bias is obtained at radii closer than half a hypercolumn. At that distance the average effect is much lower. Changing the orientation tuning of the source cells has a major influence on the directional bias. For a $HWHH$ of 20°, which is 10° less than the one currently used and similar to that of cortical simple cells, the directional bias is nearly doubled.

This result shows that entirely isotropic connections (i.e., circular inhibition) can result in a rather strong anisotropic (i.e., directionally tuned) behavior. This effect is not an artifact of the straight-column structure because, for realistically curved columns (e.g., Fig. 12) and for the real cortical patch shown in Fig. 8, a directional bias with similar strength (<10% change) is obtained (data not shown).

DISCUSSION

The purpose of this work is to provide insight into the functional limitations of long-range interactions generated by structural elements in the cortex. We used the standard structural cross-orientation inhibition as an example to show that long-range mechanisms can result in unwanted functional asymmetries (Figs. 1–3). We proposed a new mechanism called circular inhibition, which is less strongly subjected to structural limitations and fits better to the experimentally observed tuning of inhibition.[9] In addition, this mechanism resulted in an unexpected directional bias. It should be realized at this point that circular inhibition can be regarded as a simple, analytically treatable limit case for long-range lateral inhibitory connections in a two-dimensional system. This simple scheme is certainly not an accurate description of the complicated cortical network, but we found that it could capture several results from cortical physiology. We will now try to generalize our observations about the effect of long-range interactions on cortical orientation selectivity and make more general statements about basic interactions between structure and function that impose restrictions on long-range connections.

Assumptions used in the structurally confined model

This study focused entirely on structural elements in the visual cortex and their interactions with each other. "Structural elements," however, are defined in many levels; some of these are purely anatomic, whereas others describe the functional anatomy (e.g., orientation columns, ocular dominance columns, etc.). So far it proved to be very difficult to draw conclusions between the low-level (e.g., anatomic) structure and the function of cells (Braitenberg 1985; Eccles 1984; Martin 1988). In fact, some of the most straightforward assumptions turned out to be wrong (e.g., the orientation of the dendritic tree is not related to the orientation preference of the cells) (Martin and Whitteridge 1984; but see Tieman and Hirsch 1982, 1985). Therefore we chose the approach of trying to establish links between higher-level structural elements (orientation columns) and their actual function (orientation selectivity).

In this study, as opposed to a previous report (Wörgötter and Koch 1991) wherein a more complex model was presented, we stripped the cells of all properties but their orientation selectivity. The cells were embedded in different cortical column structures, from the very simple to realistic. In doing so, many complications were removed that certainly also affect the behavior of real cells. For instance, all cells had identical receptive fields and only the preferred orientation was varied. In the spatial domain, only linear interactions were assumed between receptive fields (Figs. 2 and 4). No temporal interactions were implemented (see Wörgötter and Holt 1991 for a different approach). As was noted in the INTRODUCTION, we consider this simplicity a desired feature of our model and not a fault. By reducing the detailed cortex model to all but the essential features, we were able to understand the intriguing observations about functional cross-orientation inhibition and about the generation of a directional bias (Wörgötter and Koch 1991).

Structural cross-orientation inhibition

Structural cross-orientation inhibition has been suggested by several investigators (Benevento et al. 1972; Bishop et al. 1973; Burr et al. 1981; Creutzfeldt et al. 1974; Hess and Murata 1974; Matsubara et al. 1985, 1987; Morrone et al. 1982; Sillito 1975, 1979; Sillito et al. 1980; Tsumoto et al. 1979) as a mechanism to sharpen orientation selectivity in cortical cells. This study showed that the efficiency of structural cross-orientation inhibition is limited due to the structure of the orientation columns. Note that the restrictions of structural cross-orientation inhibition shown in Figs. 1–3 are not eliminated by making the model more realistic. Even taking into account cortical magnification, receptive-field scatter and overlap, as well as orientation jitter, this type of rigidly defined cross-orientation inhibition will only work optimally if the receptive-field centers of the connected cells are identical, which is not the general case. Several ways exist to implement structural cross-orientation inhibition in a broader sense: one can vary the angle between preferred orientation and the connection axis by wiring together cells with <90° orientation difference, or one can select different connection distances. With the existing knowledge of the relations be-

---

[9] For a discussion on other possible (short and long-range) connection schemes see Wörgötter and Koch (1991). This paper also treats more realistic "circular" and "disk-like" connection patterns, where connections arise from cells not only on a perimeter.

tween cortical anatomy and physiology, neither of the above modifications can be ruled out conclusively. All these modifications, however, have in common that they raise the level of specificity of the connection scheme. As already mentioned in the INTRODUCTION, specificity in excitation can be generated rather easily with Hebb-type mechanisms, which, however, do not work for inhibitory connections. In addition, recent evidence suggests that the tuning of functional cross-orientation inhibition is rather weak (Bonds 1989; Eysel and Wörgötter 1991). We suggest, therefore, a different, more broadly tuned mechanism, which we call circular inhibition.

Circular inhibition

This study showed that circular inhibition results in a net functional cross-orientation inhibition effect at a radius of about half a hypercolumn. The tuning curves show that the effect is probably not very strong. However, it is necessary to keep in mind that the "tuning of inhibition" curves do not allow for extrapolation of the actual orientation tuning bandwidth of the cells, because this is crucially influenced by the inhibitory action (e.g., subtractive vs. divisive). Nevertheless, the rather weak tuning of inhibition is in agreement with experimental results. Because in the detailed simulation (Wörgötter and Koch 1991) no specific tuning of inhibition was observed when the inhibitory cells were located on the complete disk surrounded by the circle, it is conceivable that the level of specificity in circular inhibition is close to the lower limit at which any specific effect in the cortical structure can be obtained.

It should be noted that circular inhibition implemented with constant "synaptic weights" on the whole circle (as is here) and without a threshold yields some degree of end-stopping (Hubel and Wiesel 1965). Although end-stopping is a very common feature in cortical cells, it is not found in all of them. Orban (1984) gives the percentage of end-stopped cells to be 36–63% in areas 17–19. However, as soon as circular inhibition is implemented with a threshold, the majority of the cells do not show significant end-stopping. This is because, in most cases, the inhibitory elements that act along the long axis of the receptive field of the center cell (and which would produce end-stopping) will be nonoptimally oriented and consequently remain subthreshold. In general, thresholding proved to be a very efficient and plausible addition to our mechanism and greatly sharpened orientation tuning. A second conceivable possibility that avoids end-stopping is the implementation of circular inhibition with different weights along different directions. This would increase the specificity of the mechanism (i.e., increase the orientation tuning of the target cell) and eliminate end-stopping if the weights along the respective axis are small. Of course, the term circular inhibition is questionable when used in conjunction with this circuitry. Even these cells might, however, go through a developmental stage in which they receive circular inhibition in a strict sense. Circular inhibition is advantageous during neural development, because only distance information is required to make the necessary connections. In addition, later in development, elimination of inhibitory synapses can be

achieved much more easily than by a specific strengthening (for a review see Fregnac and Imbert 1984).

An interesting but not entirely unexpected result was the change from functional iso- to cross- to isoorientation effects with increasing radius. Matsubara et al. (1985, 1987) found a distance between patches in their labeling experiment of about half a hypercolumn. They interpret their results in terms of inhibition. Using similar labeling methods, Gilbert and Wiesel (1989) demonstrate patchy connections between isooriented cell clusters at a distance of a full hypercolumn. These are not necessarily contradictory results, because according to our observations, two connection schemes could coexist: inhibition in a distance $\lambda/2$ and excitation in a distance λ. Both act similarly and both contribute to sharpen the orientation tuning of the respective target. The multitude of studies that support the different connection schemes suggests a coexistence of them [short- or long-range isoorientation inhibition: Blakemore and Tobin 1972; DeValois et al. 1982; Ferster 1986, 1987; (Heggelund 1981, receptive fields can be nonoriented) Sillito 1979; structural cross-orientation inhibition: Benevento et al. 1972; Bishop et al. 1973; Burr et al. 1981; Creutzfeldt et al. 1974; Hess and Murata 1974; Morrone et al. 1982; Sillito 1975, 1979; Sillito et al. 1980; Tsumoto et al. 1979; Eysel and Wörgötter 1991; long-range isoorientation excitation: Gilbert 1985; Gilbert and Wiesel 1983; Nelson and Frost 1985; Rockland and Lund 1982, 1983; Ts'o et al. 1986; long-range isoorientation inhibition: Eysel et al. 1988]. It remains unclear whether inhibition is transmitted directly (via long axons) or excitatory cells converge onto local inhibitory interneurons, resulting in the same effect.

Generation of a directional bias

The generation of a directional bias with circular inhibition was the most intriguing and unexpected finding in the detailed cortex model. In the present study, it is shown that circular inhibition, although apparently isotropic, will for most cells result in a directional bias. This bias is an inherent feature of the column structure and the connection scheme and it is not introduced by noise-induced symmetry breaking. The degree of directional tuning achieved this way is lower than the one observed in cortical cells. It is, however, tempting to speculate that this bias triggers the development of more specific mechanisms, with the final result of the strong direction selectivity found in cortical cells.

Concepts for long-range interactions

In this paper, we studied how sharpening of orientation selectivity is achieved by the connections between cells. The visual cortex is functionally isotropic for distances smaller than 0.2 mm (Albus 1975a). Isotropy means here that within this distance, no predictions can be made about the efficiency of a connection in any direction, regardless of the orientation preference of the target cell. As shown in Fig. 1, this changes at larger distances. Here, the efficiency of geometrically identically arranged connections changes with

the orientation preference of the target cell. We believe that this anisotropy poses a general problem on all long-range connection schemes. Either long-range connections have to be designated very specifically to their task, or the connection scheme has to be so general (like circular inhibition) that it results in only negligible conflict with the underlying structure. A geometrically defined connection scheme of "intermediate" specificity (like structural cross-orientation inhibition) will not perform equally well at all locations, because of its interference with the geometry of the column structure. As discussed above, Hebb mechanisms can account for high specificity in excitatory interactions. For inhibitory connections one should consider the possibility that development has chosen the second (the unspecific) solution.

Conclusion

Understanding the relationship between structure and function in the visual cortex is a fundamental requirement for the understanding of the signal processing that takes place in this part of the brain. The low anatomic order in the cortex, however, makes it even more complicated to draw rigorous links between structure and function. Many of the (older) studies on the visual cortex were therefore confined to a description of either structural or functional aspects. Despite the availability of modern experimental and modeling methods, the understanding of the link between structure and function is still far from perfect. Most experimental studies are paired with qualitative models, whereas many quantitative models only weakly rely on the physiological data. Our modeling approaches tried to gain insight in the relationship between structure and function in the visual cortex elaborating the results from a detailed simulation (Wörgötter and Koch 1991) with a more readily discernible, structurally confined approach in the current study. We were able to explain the phenomena we observed in the detailed model and it was possible to shine a light on the role of structural specificity of long range connections. In particular, we could show that an unspecific and isotropic mechanism (circular inhibition) can produce specific and anisotropic behavior.

APPENDIX A

Analytical description of cortical orientation columns

It is not known in detail how the orientation preference varies along the cortical surface. We will present in the following a simple, but quantitative, model, which contains the essential features of cortical columns (smooth transients, hypercolumns, singularities, etc.). The model is purely descriptive; we are not at all concerned with the development of the cortex.

Our model is a straightforward generalization of an idea put forward by Swindale (1985). He represented the orientation preference of a given cell by a vector $\vec{z}$ in the cortical plane. We define the preferred orientation of the cell by

$$\phi = \arctan \frac{z_y}{z_x} \qquad (A1)$$

where z_x and z_y are the x and y components of $\vec{z}$, respectively.[10] An important special case, which has been treated in more detail in APPENDIX B (see Eq. B1), is $z_x = \cos(\pi/\lambda x)$, $z_y = \sin(\pi/\lambda x)$, from which follows

$$\phi = \arctan \frac{\sin(\pi/\lambda x)}{\cos(\pi/\lambda x)} = \frac{\pi}{\lambda} x \qquad (A2)$$

where λ is the width of one hypercolumn. All orientations appear over a distance of λ along the hypercolumn (i.e., in this model, along the x-axis), as is required by the definition of a hypercolumn (Hubel and Wiesel 1963).

Equation A2 can be generalized to

$$\phi = \arctan \frac{\sum_{i=1}^{N} [\sin(k_i x + l_i y)]}{\sum_{i=1}^{N} [\cos(k_i x + l_i y)]} \qquad (A3)$$

where

$$\lambda^2(k_i^2 + l_i^2) = \pi^2 \quad \text{for all} \quad i = 1, \ldots, n$$

Obviously, Eq. A2 is the special case $n = 1$ of Eq. A3. This yields parallel, straight orientation columns. A similar structure is obtained for $n = 2$ (not shown). For $n = 3$, the column structure in Fig. 12 is obtained, which shows a resemblance to real cortex. The scale of this figure has been compressed compared with Fig. 7 to show a larger part of the cortex, and longer lines have been used for each cell to show better the bent structure of the orientation columns. In particular, the following three conditions, which seem to characterize (at least partially) the cortical areas 17 and 18 of cat, are satisfied by this model cortex. 1) All cells in the cortex are a priori equivalent with respect to their location in the orientation column structure. 2) Orientations change continuously, except for isolated singularities. This corresponds to the findings that abrupt orientation changes are rarely found in a real cortex (Albus 1975b; Blasdel and Salama 1986). 3) The distribution of orientations is approximately constant over a distance of one hypercolumn. This last condition is only valid along certain directions, as well in our model as in real cortex (Swindale et al. 1987).

The major drawback of the description given by Eq. A3 is that it relies on too few data. Unfortunately, only Swindale et al. (1987) give a detailed description of a larger patch of the cortical surface. Column structures measured by others are either too small (Albus 1975b) or the measurement of the orientation preference is too coarse (Blasdel and Salama 1986). In particular, the column structure of the monkey (which contains "blobs"; Livingstone and Hubel 1984) might be arranged differently (Braitenberg 1985; Braitenberg and Braitenberg 1979; see Götz 1988) and require a different description. Nevertheless, features 1–3 demonstrate that our model captures many of the components included in different models of orientation columns systems proposed by others (Baxter and Dow 1989; Braitenberg and Braitenberg 1979; Götz 1987, 1988; von Seelen 1970). At least, it does capture all essential features relevant to the present study and it has been shown that this simple model yields results that are comparable with those obtained by the use of the columnar structure that was determined experimentally by Swindale et al. (1987).

---

[10] The angle ϕ defined in Eq. A1 varies between $-\pi/2$ and $\pi/2$, i.e., over a range of 180°, as is expected for an orientation angle. If, for some reason, negative angles are undesirable, $\pi/2$ may be added to ϕ, without changing any of the following arguments.

APPENDIX B

Circular inhibition in parallel linear orientation columns: exact results

A model cortex with parallel, straight orientation columns is shown in Figs. 1A and 7C. We assume a one-to-one projection from the visual field to the cortex, and we choose a coordinate system in the cortical plane such that the orientation columns are parallel to the y-axis (vertical in Figs. 1A and 7C). Let $\phi(x, y)$ be the angle between the preferred orientation of the cell located at (x, y) and the x-axis. In the chosen coordinate system, ϕ depends only on x. We assume that $\phi(x)$ is given by Eq. A2, i.e.

$$\phi(x) = \frac{\pi}{\lambda} x \qquad (B1)$$

where λ is the width of one hypercolumn. This yields a periodical column structure with periodicity λ, because orientation angles are defined modulo π. If a δ-function bar with an angle γ relative to the x-axis is placed over the receptive field of a cell with preferred orientation ϕ, the response of this cell (measured, e.g., in spikes per second) is assumed to be

$$A(\gamma - \phi) = A_0 + A_2 \cos(2\gamma - 2\phi) \qquad (B2)$$

as in Eq. 1 of the text. In this equation, $A_0 > A_2$ is assumed, which assures that $A > 0$.

In our model, a given cell receives inhibition from all cells on a circle with radius r, which is centered on the cell under study. If a δ-function stimulus bar with an angle γ relative to the x-axis is placed across the center of the receptive field of the cell at (x, y), this cell receives inhibitory input proportional to

$$I_\phi(x) = A[\gamma - \phi(x + r\cos\gamma)] + A[\gamma - \phi(x - r\cos\gamma)] \qquad (B3)$$

In Fig. 5, the center cell receives inhibitory input from the cells 2 and 5 for a stimulus bar with angle γ. The sum of the contributions from these two cells (which correspond to the 2 terms on the right side of Eq. B3) is depicted by the diagonal line (labeled "2 + 5") in Fig. 5C.

Using Eqs. B1 and B2, Eq. B3 is rewritten as

$$I_\phi(x) = 2A_0 + A_2 \cos\left(2\gamma - 2\frac{\pi}{\lambda}x\right)\cos\left(2\frac{\pi}{\lambda}r\cos\gamma\right) \qquad (B4)$$

To calculate the population average of the inhibitory input, we transform I_ϕ in the reference system of the cell at (x, y). Geometrically, this corresponds to a rotation by the angle ϕ, so that all center cells have a common preferred orientation of $0°$. This yields

$$I(x) = 2A_0 + A_2 \cos(2\gamma)\cos\left[2\frac{\pi}{\lambda}r\cos\left(\gamma - \frac{\pi}{\lambda}x\right)\right] \qquad (B5)$$

where γ is now relative to ϕ.

The population average for a stimulus angle γ and a radius of inhibition of r is obtained as

$$\tilde{I}(r, \gamma) = \frac{1}{\lambda}\int_0^\lambda I(x)dx = 2A_0 - A_2 J_0(2\pi r/\lambda)\cos(2\gamma) \qquad (B6)$$

where J_0 is the Bessel function of order zero.

The polar plot in Fig. 7C shows $\tilde{I}(\lambda/2, \gamma)$ as function of γ. It is seen that inhibition in the nonpreferred orientation is stronger than in the preferred orientation.

Curve C in Fig. 10 presents $\tilde{I}(r, \pi/2)/\tilde{I}(r, 0)$ as a function of r. This can be written as

$$\frac{\tilde{I}(r, \pi/2)}{\tilde{I}(r, 0)} = \frac{2A_0 + A_2 J_0(2\pi r/\lambda)}{2A_0 - A_2 J_0(2\pi r/\lambda)} \qquad (B7)$$

The first maximum of this function is at $r \approx 0.65\lambda$, and the first two minima are at $r = 0$ and at $r \approx 1.125\lambda$, respectively.

REFERENCES

ALBUS, K. A quantitative study of the projection area of the central and the paracentral visual field in area 17 of the cat. I. The precision of the topography. *Exp. Brain Res.* 24: 159–179, 1975a.

ALBUS, K. A quantitative study of the projection area of the central and the paracentral visual field in area 17 of the cat. II. The spatial organization of the orientation domain. *Exp. Brain Res.* 24: 181–202, 1975b.

BATSCHELET, E. *Circular Statistics in Biology.* London: Academic, 1981.

BAXTER, W. T. AND DOW, B. M. Horizontal organization of orientation selective cells in primate visual cortex. *Biol. Cybern.* 61: 171–182, 1989.

BENEVENTO, L. A., O. D. CREUTZFELDT, AND KUHNT, U. Significance of intracortical inhibition in the visual cortex. *Nature Lond.* 238: 124–126, 1972.

BERMAN, N. E. J., WILKES, M. E., AND PAYNE, B. R. Organization of orientation and direction selectivity in areas 17 and 18 of cat cerebral cortex. *J. Neurophysiol.* 38: 676–699, 1987.

BISHOP, P. O., COOMBS, J. S., AND HENRY, G. H. Receptive fields of simple cells in the cat striate cortex. *J. Physiol. Lond.* 231: 31–60, 1973.

BLAKEMORE, C. AND TOBIN, E. A. Lateral inhibition between orientation detectors in the cat's visual cortex. *Exp. Brain Res.* 15: 439–440, 1972.

BLASDEL, G. G. AND SALAMA, G. Voltage-sensitive dyes reveal a modular organization in monkey striate cortex. *Nature Lond.* 321: 579–585, 1986.

BLOMFIELD, S. Arithmetical operations performed by nerve cells. *Brain Res.* 69: 115–124, 1974.

BONDS, A. B. Role of inhibition in the specification of orientation selectivity of cells in the cat striate cortex. *Visual Neurosci.* 2: 41–55, 1989.

BRAITENBERG, V. Charting the visual cortex. In: *Cerebral Cortex,* edited by A. Peters and E. G. Jones. New York: Plenum, 1985, vol. 3, p. 379–414.

BRAITENBERG, V. AND BRAITENBERG, C. Geometry of orientation columns in the visual cortex. *Biol. Cybern.* 33: 179–186, 1979.

BURR, D., MORRONE, C., AND MAFFEI, L. Intra-cortical inhibition prevents simple cells from responding to textured visual patterns. *Exp. Brain Res.* 43: 455–458, 1981.

CASAGRANDE, V. A. AND NORTON, T. T. The lateral geniculate nucleus: a review of its physiology and function. In: *The Neural Basis of Visual Function,* edited by A. Leventhal. New York: Macmillan. In press.

CREUTZFELDT, O. D., KUHNT, U., AND BENEVENTO, L. A. An intracellular analysis of visual cortical neurones to moving stimuli: responses in a co-operative neuronal network. *Exp. Brain Res.* 21: 251–274, 1974.

DEVALOIS, R. L., YUND, E. W., AND HEPLER, N. The orientation and direction selectivity of cells in macaque visual cortex. *Vision Res.* 22: 531–544, 1982.

ECCLES, J. C. The cerebral neocortex: a theory of its operation. In: *Cerebral Cortex: Functional Properties of Cortical Cells,* edited by E. G. Jones and A. Peters. New York: Plenum, 1984, vol. 2, p. 1–36.

ENROTH-CUGELL, C. AND ROBSON, J. G. The contrast sensitivity of retinal ganglion cells of the cat. *J. Physiol. Lond.* 187: 517–552, 1966.

EYSEL, U. TH., MUCHE, T., AND WÖRGÖTTER, F. Lateral interactions at direction-selective striate neurones in the cat demonstrated by local cortical inactivation. *J. Physiol. Lond.* 399: 657–675, 1988.

EYSEL, U. TH., AND WÖRGÖTTER, F. Horizontal intracortical contribu-

tions to functional specificity in cat visual cortex. In: *Proceedings Schloss Ringberg Conf.*, edited by A. Aertsen and V. Braitenberg. Berlin: Springer-Verlag. In press.

FERSTER, D. Orientation selectivity of synaptic potentials in neurons of cat primary visual cortex. *J. Neurosci.* 6: 1284–1301, 1986.

FERSTER, D. Origin of orientation-selective EPSPs in simple cells of cat visual cortex. *J. Neurosci.* 7: 1780–1791, 1987.

FERSTER, D. AND KOCH, C. Neuronal connections underlying orientation selectivity in cat visual cortex. *Trends Neurosci.* 10: 487–492, 1987.

FREGNAC, Y. AND IMBERT, M. Development of neuronal specificity in primary visual cortex of cat. *Physiol. Rev.* 64: 325–434, 1984.

GILBERT, C. D. Horizontal integration in the neocortex. *Trends Neurosci.* 8: 160–165, 1985.

GILBERT, C. D. AND WIESEL, T. N. Clustered intrinsic connections in cat visual cortex. *J. Neurosci.* 3: 1116–1133, 1983.

GILBERT, C. D. AND WIESEL, T. N. Columnar specificity of intrinsic horizontal and corticocortical connections in cat visual cortex. *J. Neurosci.* 9: 2432–2442, 1989.

GÖTZ, K. G. Do "d-blob" and "l-blob" hypercolumns tessellate the monkey visual cortex? *Biol. Cybern.* 56: 107–109, 1987.

GÖTZ, K. G. Cortical templates for the self-organization of orientation-specific d- and l-hypercolumns in monkeys and cats. *Biol. Cybern.* 58: 213–223, 1988.

HEBB, D. O. *The Organization of Behavior.* New York: Wiley, 1949.

HEGGELUND, P. Receptive field organization of simple cells in cat striate cortex. *Exp. Brain Res.* 42: 89–98, 1981.

HESS, R. AND MURATA, K. Effects of glutamate and GABA on specific response properties of neurones in visual cortex. *Exp. Brain Res.* 21: 285–297, 1974.

HUBEL, D. H. AND WIESEL, T. N. Receptive fields, binocular interaction and functional architecture in the cat's visual cortex. *J. Physiol. Lond.* 160: 106–154, 1962.

HUBEL, D. H. AND WIESEL, T. N. Shape and arrangement of columns in cat's striate cortex. *J. Physiol. Lond.* 165: 559–568, 1963.

HUBEL, D. H. AND WIESEL, T. N. Receptive fields and functional architecture in two non-striate visual areas (18 and 19) of the cat. *J. Neurophysiol.* 28: 229–289, 1965.

HUBEL, D. H. AND WIESEL, T. N. Sequence regularity and geometry of orientation columns in the monkey striate cortex. *J. Comp. Neurol.* 158: 267–294, 1974.

KAMMEN, D. M. AND YUILLE, A. L. Self organizing neural networks: Hebbian learning in development and biological computing. In: *Advances in Control Networks and Large-Scale Parallel Distributed Processing*, edited by M. Fraser. Norwood, NJ: Ablex, 1991, p. 1–57.

KATO, H., BISHOP, P. O., AND ORBAN, G. A. Hypercomplex and the simple/complex cell classifications in cat striate cortex. *J. Neurophysiol.* 41: 1071–1095, 1978.

LIVINGSTONE, M. S. AND HUBEL, D. H. Anatomy and physiology of a color system in the primate visual cortex. *J. Neurosci.* 4: 309–366, 1984.

MARTIN, K. A. C. From single cells to simple circuits in the cerebral cortex. *Q. J. Exp. Physiol.* 73: 637–702, 1988.

MARTIN, K. A. C. AND WHITTERIDGE, D. The relationship of receptive field properties to the dendritic shape in the cat striate cortex. *J. Physiol. Lond.* 356: 291–302, 1984.

MATSUBARA, J. A., CYNADER, M. S., AND SWINDALE, N. V. Anatomical properties and physiological correlates of the intrinsic connections in cat area 18. *J. Neurosci.* 7: 1428–1446, 1987.

MATSUBARA, J., CYNADER, M., SWINDALE, N. V., AND STRYKER, M. P. Intrinsic projections within visual cortex: evidence for orientation-specific local connections. *Proc. Natl. Acad. Sci. USA* 82: 935–939, 1985.

MORRONE, M. C., BURR, D. C., AND MAFFEI, L. Functional implications of cross-orientation inhibition of cortical visual cells. I. Neurophysiological evidence. *Proc. R. Soc. Lond. B Biol. Sci.* 216: 335–354, 1982.

NELSON, J. I. AND FROST, B. J. Intracortical facilitation among co-oriented, co-axially aligned simple cells in cat striate cortex. *Exp. Brain Res.* 61: 54–61, 1985.

ORBAN, G. A. *Neuronal Operations in the Visual Cortex.* Berlin: Springer-Verlag, 1984.

ROCKLAND, K. AND LUND, J. Widespread periodic intrinsic connections in the tree shrew visual cortex. *Science Wash. DC* 215: 1532–1534, 1982.

ROCKLAND, K. AND LUND, J. Intrinsic laminar lattice connections in primate visual cortex. *J. Comp. Neurol.* 216: 303–318, 1983.

SCHWARTZ, E. L. Spatial mapping in the primate sensory projection: analytic structure and relevance to perception. *Biol. Cybern.* 25: 181–194, 1977.

SCHWARTZ, E. L. Computational anatomy and functional architecture of striate cortex: a spatial mapping approach to perceptual coding. *Vision Res.* 20: 645–669, 1980.

SEELEN, W. VON. Zur Informationsverarbeitung im visuellen System der Wirbeltiere. II. *Kybernetik* 7: 89–106, 1970.

SILLITO, A. M. The contribution of inhibitory mechanisms to the receptive field properties of neurones in the striate cortex of the cat. *J. Physiol. Lond.* 250: 305–329, 1975.

SILLITO, A. M. Inhibitory mechanisms influencing complex cell orientation selectivity and their modification at high resting discharge levels. *J. Physiol. Lond.* 289: 33–53, 1979.

SILLITO, A. M., KEMP, J. A., MILSON, J. A., AND BERARDI, N. A re-evaluation of the mechanisms underlying simple cell orientation selectivity. *Brain Res.* 194: 517–520, 1980.

SOMOGYI, P., KISVÁRDAY, Z. F., MARTIN, K. A. C., AND WHITTERIDGE, D. Synaptic connections of morphologically identified and physiologically characterized large basket cells in the striate cortex of the cat. *Neuroscience* 10: 261–294, 1983.

SWINDALE, N. V. Iso-orientation domains and their relationship with cytochrome oxidase patches. In: *Models of the Visual Cortex*, edited by D. Rose and V. G. Dobson. New York: Wiley, 1985, p. 452–461.

SWINDALE, N. V., MATSUBARA, J. A., AND CYNADER, M. S. Surface organization of orientation and direction selectivity in cat area 18. *J. Neurosci.* 7: 1414–1427, 1987.

THIBOS, L. N. AND LEVICK, W. R. Orientation bias of brisk transient Y-cells of the cat retina for drifting and alternating grating. *Exp. Brain Res.* 58: 1–10, 1985.

TIEMAN, S. B. AND HIRSCH, H. V. B. Exposure to lines of only one orientation modifies dendritic morphology of cells in the visual cortex of the cat. *J. Comp. Neurol.* 211: 353–362, 1982.

TIEMAN, S. B. AND HIRSCH, H. V. B. Role of dendritic field in orientation selectivity. In: *Models of the Visual Cortex*, edited by D. Rose and G. Dobson. New York: Wiley, 1985, pp. 432–443.

TS'O, D. Y., GILBERT, C. D., AND WIESEL, T. N. Relationships between horizontal interactions and functional architecture in cat striate cortex as revealed by cross correlation analysis. *J. Neurosci.* 6: 1160–1170, 1986.

TSUMOTO, T., ECKART, W., AND CREUTZFELDT, O. D. Modification of orientation selectivity of cat visual cortex neurons by removal of GABA mediated inhibition. *Exp. Brain Res.* 34: 351–363, 1979.

TUSA, R. J., PALMER, L. A., AND ROSENQUIST, A. C. The retinotopic organization of area 17 (striate cortex) in the cat. *J. Comp. Neurol.* 177: 213–236, 1978.

TUSA, R. J., ROSENQUIST, A. C., AND PALMER, L. A. The retinotopic organization of area 18 and 19 in the cat. *J. Comp. Neurol.* 185: 657–678, 1979.

WÖRGÖTTER, F., AND EYSEL, U. TH. Quantitative determination of orientational and directional components in the response of visual cortical cells to moving stimuli. *Biol. Cybern.* 57: 349–355, 1987.

WÖRGÖTTER, F., GRÜNDEL, O., AND EYSEL, U. TH. Comparison of cell properties in cat's striate cortex determined by different types of stimuli. *Eur. J. Neurosci.* 2: 928–941, 1990.

WÖRGÖTTER, F. AND HOLT, G. Spatiotemporal mechanisms in receptive fields of visual cortical simple cells: a model. *J. Neurophysiol.* 65: 494–510, 1991.

WÖRGÖTTER, F. AND KOCH, C. A detailed model of the primary visual pathway in the cat. Comparison of afferent excitatory and intracortical inhibitory connection schemes for orientation selectivity. *J. Neurosci.* In press.